

# A dynamical study of fission process and estimation of pre-scission neutron multiplicity

Asish K. Dhara, Kewal Krishan, Chandana Bhattacharya\* and Sailajananda Bhattacharya  
*Variable Energy Cyclotron Centre, 1/AF Bidhan Nagar, Calcutta- 700 064, India*

The dynamics of fission has been studied by solving Euler-Lagrange equations with dissipation generated through one and two body nuclear friction. The average kinetic energies of the fission fragments, pre-scission neutron multiplicities and the mean energies of the pre-scission neutrons have been calculated and compared with experimental values and they agree quite well. A single value of friction coefficient has been used to reproduce the experimental data for both symmetric and asymmetric splitting of the fissioning systems over a wide range of masses and excitation energies. It has been observed that a stronger friction is required in the saddle to scission region as compared to that in the ground state to saddle region.

## I. INTRODUCTION

The studies of fission dynamics has become a subject of current interest due to availability of recent experimental data for pre-scission neutron multiplicities in heavy ion induced fusion-fission reactions [1–10]. From the analysis of the data, it is by and large established that standard statistical theory could not account for the observed large multiplicity of the pre-scission neutrons. This discrepancy is, nowadays, believed to be of dynamical origin, and thus led to enormous activities to understand theoretically the dynamics of fission process [11–22].

Dynamics of fission consists in the study of gradual change of shape of a fissioning compound nucleus. The shape is globally characterised in terms of elongation parameter, the neck radius and mass ratio of two fragments. These variables are usually referred to as collective variables and dynamics is understood in terms of the evolution of these collective variables. It has been observed that time taken by the compound nucleus from its state of formation to the state when it gets dissociated into the two fragments is 'too short' when the shape evolves under the effect of the conservative forces derived from the Coulomb and surface energy of the compound nucleus. With the average neutron evaporation rate determined by excitation of the compound nucleus, such large pre-scission neutron multiplicity data can not be explained in any manner with this 'short' time scale of fission process. This feature leads one to believe that the dynamical process of shape evolution gets inhibited for a considerable amount of time. This retardation in the dynamics of collective variables is effected through a mechanism of dissipation by assuming the fissioning nucleus as a liquid drop. The dissipation is usually realised by introducing a friction term in the dynamics of shape evolution. Thus, the explanation of the observed large neutron multiplicity points to two important features of the fission process; the time scale of fission and the viscosity of the nuclear fluid. The dynamics of fission is then picturised as a dissipative process where initial energy of the collective variables get dissipated into the internal degrees of freedom of nuclear fluid giving rise to the increase in internal excitation energy, which, in turn, is responsible for the evaporation of pre-scission neutrons.

There have been different approaches to study this problem. One approach is to solve the Langevin equations for the collective variables [11,12,14,15]. In this approach, one assumes the collective variable as the 'Brownian particle' interacting stochastically with large number of internal degrees of freedom constituting the surrounding 'bath'. The systematic dissipative force is assumed to be derived from the random force averaged over a time larger than the collisional time scale between collective and internal degrees of freedom. The random part is modelled as a gaussian white noise which causes the fluctuation of the physical observables of the fission process such as kinetic energies, yields of the fission fragments etc. In the other approach, one solves the multi-dimensional Fokker-Planck equation [16–18], which is a differential version of Langevin equation. In both of these approaches, the calculated average kinetic energies, average yield of the fission fragments and neutron multiplicity compare more or less well with the respective experimental data.

Following an alternative approach, we proposed a dynamical model of fission [21,22], which could explain fairly well various features observed in fusion-fission reactions of lighter systems. In that model, we solved the Euler-Lagrange equations for the collective variables instead of solving the Fokker-Planck or Langevin equations. The fluctuations are introduced at the initial level of the dynamics by random partitioning of available energy of the 'nascent' compound nucleus between the collective and the intrinsic degrees of freedom and attributing the former to the generator of the displacement of the collective variable as an initial condition of Euler-Lagrange equation. The random initial

momentum given to the collective variable gives rise to different trajectories. Some of these trajectories would cross the fission barrier and have the 'fission fate'. The main difference between our approach and those of the others is that in our approach the dynamics is deterministic with randomisation at initial level, while in other approaches, the dynamics is mainly stochastic in nature. However, in all these approaches the dissipation is introduced in terms of frictional forces.

In our earlier calculations [21,22] we assumed a schematic shape of the fissioning system which comprised of two leptodermous spheres connected by a cylindrical neck. This particular idealisation was introduced by Swiatecki [23] to simplify the calculation of various ingredients such as conservative forces etc. After the saddle point, the neck gets constricted and at the scission point the spheres get detached forming two fission fragments. The calculation with such simple shape produced results which agree quite well with the experimental data, particularly for the nuclei lying below the Businaro-Gallone point. It is, however, known that for heavy nuclei lying above the Businaro-Gallone point, the fission shapes are highly deformed, and elongation is quite large before the nucleus reaches the scission point. Obviously, the simple schematic shape parametrisation [23] used earlier would not be expected to mimic such large deformed shapes. Besides, the dissipation of collective energy to the internal nucleonic degrees of freedom could happen through two different mechanisms. One is due to two-body collision of the nucleons inside the nuclear fluid, the other is due to collision of nucleons with changing surface of the nuclear fluid, which is more commonly known as one-body or 'Wall' friction and both of them depend very sensitively on the surface profile of the fissioning system. Hence, with these considerations in mind, in the present paper, we have used a more realistic shape parametrisation of the heavy fissioning systems to study the temporal evolution of fission shapes, and, subsequently, to calculate various observables of the fission process, such as precission neutron multiplicities, total kinetic energies etc.

The present paper has been arranged as follows. In Sec. II we describe the model and the statistics used in calculating the average kinetic energies, precission neutron multiplicities etc. The results of the calculation are discussed in Sec. III. Finally, concluding remarks are given in Sec. IV.

## II. THE MODEL

The present model is a generalisation of the schematic model developed by us [21] to study the fusion-fission process for light nuclear systems lying below the Businaro-Gallone point. The schematic parametrisation for the evolution of fission shapes used in the earlier work has been replaced by a more realistic parametrisation for the same that is applicable for heavier nuclei with fissility parameters above the Businaro-Gallone value.

### A. The shape

The shape of the nuclear surface is assumed to be of the form

$$\rho^2(z) = c^{-2}(c^2 - z^2)(A + Bz^2 + \alpha zc), \quad (1a)$$

where the coefficients  $A$  and  $B$  are defined as

$$A = c^{-1} - B/5, \quad (1b)$$

$$B = (c - 1)/2. \quad (1c)$$

This is a specific form of the surface introduced by Brack et. al. [24]. The quantity  $c$  corresponds to the elongation and the quantity  $\alpha$  is a parameter which depends upon the asymmetry ( $a_{sym}$ ) defined below. We may note that the surface cuts the  $z$ -axis at  $z = \pm c$ , so that the surface to surface separation along the elongation axis is  $2c$ . There are three real points at which the derivative of  $\rho$  vanishes; two of them correspond to maximum of  $\rho$  and between these two maxima one minimum occurs at  $z = z_{min}$ . The portion of volume contained in  $z = -c$  to  $z = z_{min}$  is defined as left lobe and remaining portion of the volume is referred to as right lobe. Asymmetry ( $a_{asy}$ ) is then defined as

$$a_{asy} = \frac{(A_R - A_L)}{A_{CN}} \quad (2)$$

where  $A_{CN}$  is the compound nucleus mass, and  $A_R$ ,  $A_L$  correspond to the masses of the right and left lobes, respectively. The parameter  $\alpha$  is related to the asymmetry  $a_{asy}$  through the following relation

$$\alpha = .11937a_{asy}^2 + .24720a_{asy}. \quad (3)$$

As the shape changes gradually, the coordinates of the two maxima and that of the minimum change. The scission point is defined when the minimum point touches the  $z$ -axis and it is given by

$$A - \frac{c^2\alpha^2}{4B} = 0. \quad (4)$$

Therefore, the value of  $c$  at which scission occurs depends on  $\alpha$  and the dependence is given by

$$c_{sc} = -2.0\alpha^2 + .032\alpha + 2.0917. \quad (5)$$

## B. The dynamics

The dynamics is studied by calculating the semi-classical fission trajectories. The trajectories are obtained by solving the Euler-Lagrangian equation [21],

$$\mu\ddot{r} - \frac{L^2}{\mu r^3} = -\gamma_r\dot{r} - \frac{\partial(V_C + V_N)}{\partial r}, \quad (6a)$$

$$I_1\ddot{\theta}_1 = \gamma_t[g_2(\dot{\theta}_2 - \dot{\theta}) + g_1(\dot{\theta}_1 - \dot{\theta})]g_1, \quad (6b)$$

$$I_2\ddot{\theta}_2 = \gamma_t[g_2(\dot{\theta}_2 - \dot{\theta}) + g_1(\dot{\theta}_1 - \dot{\theta})]g_2, \quad (6c)$$

$$\dot{L} = -(I_1\dot{\theta}_1 + I_2\dot{\theta}_2). \quad (6d)$$

The quantities  $V_C$ ,  $V_N$  represent the Coulomb and nuclear interaction potentials and  $\gamma_r$ ,  $\gamma_t$  are the radial and tangential components of friction, respectively.  $I_1, I_2$  are the moments of inertia of the two lobes and  $L$  refers to the relative angular momentum.  $g_1$  and  $g_2$  are the distances of the centres of mass of the two lobes from the centre of mass of the composite dinuclear system and the term  $[g_2(\dot{\theta}_2 - \dot{\theta}) + g_1(\dot{\theta}_1 - \dot{\theta})]$  represents the relative tangential velocity of the two lobes [21]. The variable  $r$  is defined as the centre to centre distance between the two lobes. From the generalised shape given by Eqn. 1a, we first construct the centres of mass of left and right lobes, and call them  $z_l$  and  $z_r$  respectively. Then  $r$  is defined as

$$r = |z_l - z_r|. \quad (7)$$

The reduced mass parameter  $\mu$ , is obtained from the calculated masses of the two lobes.

For the non-conservative part of the interaction, we would consider viscous drag arising not only due to two body collision but also due to the collisions of the nucleons with the wall or surface of the nucleus. Hence  $\gamma_r$  in Eqn. 6a contains two parts;  $\gamma_r^{TB}$  and  $\gamma_r^{OB}$ , for two-body and one-body dissipative mechanisms, respectively. Assuming the nucleus as an incompressible viscous fluid, and for nearly irrotational hydrodynamical flow,  $\gamma_r^{TB}$  is calculated by use of the Werner-Wheeler method [19,20] and is given by

$$\gamma_r^{TB} = \pi\mu_0 R_{CN}f(\partial c/\partial x) \int_{-c}^{+c} dz\rho^2[3A_c'^2 + \frac{1}{8}\rho^2 A_c''^2] \quad (8a)$$

where

$$A_c(z) = -\frac{1}{\rho^2(z)} \frac{\partial}{\partial c} \int_{-c}^z dz'\rho^2(z'). \quad (8b)$$

The quantities  $A_c', A_c''$  are the first and second derivatives of  $A_c(z)$  with respect to  $z$ .  $\mu_0$  is the two body viscosity coefficient. The factor  $f(\frac{\partial c}{\partial x})$  is taken to be

$$f(\frac{\partial c}{\partial x}) = (\frac{\partial c}{\partial x})^2 + 2(\frac{\partial c}{\partial x}), \quad (9)$$

where  $x = r/R_{CN}$ ,  $R_{CN}$  being the radius of the compound nucleus. This factor is a consequence of the rotational symmetry of the shape (1a) around the elongation axis. The variable  $r$  is already defined and the relationship between  $c$  and  $x$  is found to be

$$c = px^2 + qx + \tilde{r}(\alpha), \quad (10a)$$

where,  $p = -.15901$ ,  $q = 1.03749$ , and  $\tilde{r}$  is given by,

$$\tilde{r} = -1.228\alpha^2 - .01896\alpha + .45956. \quad (10b)$$

The tangential friction  $\gamma_t^{TB}$  is calculated using the following relation [21],

$$\gamma_t^{TB} = \left(\frac{\partial c}{\partial n}\right)^2 \gamma_r^{TB}. \quad (11)$$

The quantity  $n$  refers to the neck radius of the composite shape given by Eqn. 1a. It is defined as the value of  $\rho$  where  $\rho^2$  has a minima. The variation of  $n$  with  $c$  for different values of the parameter  $\alpha$  is shown in Fig. 1. It is evident from the figure that for all values of  $c$ , the corresponding values of  $n$  are nearly independent of  $\alpha$ , and  $n$  is found to be related to  $c$  by the following relation,

$$n = -1.047c^3 + 4.297c^2 - 6.309c + 4.073 \quad (12)$$

One body dissipative force,  $F_{dis}$ , is obtained from the rate of energy dissipation,  $E_{dis}$ , by

$$F_{dis} = -\frac{\partial}{\partial \dot{x}} E_{dis}(x) \quad (13)$$

where  $\dot{x}$  refers to the rate of change of  $x$  with respect to time and  $E_{dis}(x)$  is the rate of energy dissipation at  $x$  given by

$$E_{dis} = \frac{1}{2} \rho_m \bar{v} \oint dS \bar{e}_n^2, \quad (14)$$

where  $\bar{e}_n$  is the unit normal direction at the surface. The integration is done over the whole surface.  $\rho_m$  is the nuclear density and  $\bar{v}$  is the average nucleonic speed obtained from the formula

$$\bar{v} = \sqrt{\left(\frac{8k}{m\pi}\right)(E_{av}/a)^{1/4}} \quad (15)$$

with  $E_{av}$  is the available energy and the level density parameter,  $a$ , is taken to be  $A_{CN}/10$ . For the generalised shape (1a), one-body friction,  $\gamma_r^{OB}$ , is obtained as

$$\gamma_r^{OB} = 2\pi \rho_m \bar{v} R_{CN}^2 f(\partial c/\partial x) \int_{-c}^{+c} dz \rho [1 + \rho'^2]^{-1/2} [A_c \rho' + (1/2) \rho A'_c]^2 \quad (16)$$

where  $\rho'$ ,  $A'_c$  are the derivatives of  $\rho$ ,  $A_c$  with respect to  $z$  and all other quantities are defined earlier. The tangential friction  $\gamma_t^{OB}$  is calculated in a similar way as in Eqn. 11.

After the formation, the compound nucleus is in the minimum of the potential energy surface and it is assumed that the total initial energy available in the fusion process is equilibrated to allow the system to be described in terms of a thermodynamic state. Some part of it may be locked in rotational energy of the compound nucleus and the remaining part is the available excitation energy. However, what fraction of the available excitation energy will be converted into the collective excitation leading to the temporal evolution of fission shapes, is not known apriori. In our model, it is assumed that a random fraction of this available energy is imparted to the collective degrees of freedom which initiates the dynamics of the fission process. The initial conditions of  $r$  and  $\dot{r}$  are

$$r(t=0) = r_{min}, \quad (17a)$$

$$\dot{r}(t=0) = (E^* R_N / 2\mu)^{1/2}, \quad (17b)$$

where  $R_N$  is a random number between 0 and 1 from uniform probability distribution. The available excitation energy,  $E^*$ , is given by

$$E^* = E_{cm} + Q_{ent} - L^2/2I_{CN}, \quad (18)$$

where  $E_{cm}$  and  $Q_{ent}$  are the centre of mass energy and  $Q$ -value in the entrance channel, and,  $I_{CN}$  is the moment of inertia of the compound nucleus. The initial conditions of the angle variables at time  $t=0$  are

$$\theta(0) = \theta_1(0) = \theta_2(0) = \dot{\theta}_1(0) = \dot{\theta}_2(0) = 0, \quad (19a)$$

$$\dot{\theta}(0) = L/I_{CN} \quad (19b)$$

The dynamical evolution starts at  $r = r_{min}$ , where the minimum of the potential energy occurs. Once it reaches the saddle point or the top of the barrier, it is almost certain that it will reach the scission point.

### C. The neutron multiplicity

The emission of the pre-scission neutrons is incorporated in the present model as follows. During the temporal evolution of the fission trajectory the intrinsic excitation of the system is calculated at each time step. Correspondingly, the neutron decay width at that instant,  $\Gamma_n$ , is calculated using the relation  $\Gamma_n = \hbar W_n$ , where the decay rate  $W_n$  is given by

$$W_n = \int_0^{E_{max}} dE \frac{d^2 \Pi_n}{dE dt}. \quad (20)$$

The rate of decay  $A \rightarrow A - 1 + n$  in an energy interval  $[E, E + dE]$  and a time interval  $[t, t + dt]$ ,  $\frac{d^2 \Pi_n}{dE dt}$ , is given by

$$\frac{d^2 \Pi_n}{dE dt} = (1/\pi^2 \hbar^3) E \sigma_{inv} \mu_r \frac{\omega_{A-1}(E_{A-1}^*)}{\omega_A(E_A^*)}. \quad (21)$$

The quantity  $\omega_A(E^*)$  is the level density for the nucleus with atomic number  $A$  and excitation energy  $E^*$ .  $\sigma_{inv}$  is the inverse cross section for the reaction  $(A - 1) + n \rightarrow A$  and  $\mu_r$  is the reduced mass of  $(A - 1, n)$  system. The upper limit of integration in Eqn. 20 is given by

$$E_{max} = E^* + B_A - (B_{A-1} + B_n), \quad (22)$$

where  $B_A$  is the binding energy of the nucleus with atomic number  $A$  and  $B_n$  is the neutron separation energy. The emission of neutron in the evolution of trajectory is now conceived by fixing a criterion. We evaluate the ratio of neutron decay time  $\tau_n (= \hbar/\Gamma_n)$  and the time step  $\tau$  of the calculation. The ratio  $\tau/\tau_n$  is compared with a random number  $R_N$  from a uniform probability distribution. The criterion of emission of a neutron at random time is fixed with the rule that whenever

$$\tau/\tau_n > R_N \quad (23)$$

the emission of a neutron takes place. If condition (23) is not satisfied, no emission of neutron takes place. The probability of emission of a neutron in time  $\tau$  is  $(\tau/\tau_n)$ . The time step  $\tau$  is chosen in such a way that it satisfies the condition  $\tau/\tau_n \ll 1$ . This suggests that the evaporation is a Poisson process leading to exponential decay law with half life  $\tau_n$  [22]. Consequently the probability of emission of two or more neutrons in time  $\tau$  would be extremely small.

The kinetic energy of the emitted neutron is extracted through random sampling technique. For this purpose, it is assumed that the system is in thermal equilibrium at each instant of time  $t$ , and therefore, the energy distribution of the emitted neutrons may be represented by a normalised Boltzmann distribution corresponding to the instantaneous temperature of the system. From a uniformly distributed random number sequence  $\{x_n\}$  in the interval  $[0,1]$ , we construct another random number sequence  $\{y_n\}$  with probability distribution  $f(y)$ , where  $f(y) \sim \exp(-\beta(t)y)$  is a normalised Boltzmann distribution corresponding to the temperature  $\beta(t)$  at any instant of time  $t$ . Then, the sequence  $\{y_n\}$  is obtained from the sequence  $\{x_n\}$  by the relation,

$$y(x) = F^{-1}(x), \quad (24a)$$

where,  $F^{-1}$  is the inverse of the function  $F(y)$ , which is given by,

$$x = \int_0^y f(y) dy = F(y). \quad (24b)$$

The inverse function is computed numerically by forming a table of integral values. The energy of the emitted neutron is given by  $E_n = y E_n^{max}$ , where  $E_n^{max}$  is chosen in such a way that the Boltzmann probability at that energy is negligible for all instants of time  $t$ . After the emission of the neutron, the intrinsic excitation energy is recalculated and the trajectory is continued. In this way for each angular momentum  $l$  of the compound system, the average number of emitted neutrons per fission event  $\langle M_n \rangle_l$ , is calculated.

### D. The statistics

As argued previously, in the present model randomness is introduced only at the initial level when the compound nucleus is at the minimum of the potential energy surface. A random fraction of excitation energy is given to the

collective degrees of freedom. As a consequence, all trajectories would not be able to cross the barrier and would not have fission fate. Apart from that, there is a parameter  $\alpha$  in Eqn. 1a which decides the final asymmetry of fission fragments uniquely through Eqn. 3. For obtaining different asymmetry, one should introduce a probability distribution  $P_l(\alpha)$  at the initial level. It is natural to assume  $P_l(\alpha)$  to be proportional to the density of states available for that  $\alpha$ . Thus  $P_l(\alpha)$  is taken to be

$$P_l(\alpha) \propto u^{-2} \exp[2(au)^{1/2}] \quad (25a)$$

where  $a$  is the level density parameter and  $u$  is given by

$$u = E^* - V_{min}(\alpha) \quad (25b)$$

and  $V_{min}(\alpha)$  is the minimum of the potential energy surface for a given  $\alpha$ .

The compound nucleus is formed from the fusion process with different angular momentum. The dynamics to follow after its formation depends intricately on this angular momentum as seen from (18). Hence the probability to cross the barrier would depend upon this angular momentum. We call this probability  $P_l(f, \alpha|l)$ . This is obtained as the ratio of number of trajectories crossing the barrier for given  $\alpha$  and  $l$  and the total number of trajectories chosen. Therefore average of any observable quantity,  $O$ , is given by

$$\langle O \rangle = \frac{\sum_{l=0}^{l=l_{cr}} (2l+1) O(\alpha, l) P_l(f, \alpha|l) P_l(\alpha)}{\sum_{l=0}^{l=l_{cr}} (2l+1) P_l(f, \alpha|l) P_l(\alpha)}, \quad (26)$$

where the quantity  $O$  may be any of the relevant observables of interest, *e.g.*, kinetic energy, neutron multiplicity etc., and,  $l_{cr}$  is the critical angular momentum for fusion.

### III. RESULTS AND DISCUSSIONS.

A large amount of precision neutron multiplicity data over a wide range of excitation energies and masses of the compound nucleus is presently available in the literature. We have chosen a few representative systems in the ranges of masses  $A_{CN} \sim 150-250$ , and, excitation energies  $E_{CN}^* \sim 60-160$  MeV. All the systems considered here are above the Businaro-Gallone point and symmetric fission is the predominant mode of decay. Therefore, the theoretical predictions for various physical observables, *ie*, precision neutron multiplicities ( $n_{pre}$ ), total kinetic energies (TKE), average energies of the precision neutrons ( $\langle E_n \rangle$ ), etc., have been made for the symmetric fission and confronted with the respective data. In addition, some recent experiments have been reported where fragment mass asymmetry dependence of the related physical observables have been studied for a few of the systems mentioned above. Explanation of such exclusive data is a crucial test for any theoretical model and it has not been, to the best of our knowledge, attempted so far. Therefore, we have made calculations for the fragment mass asymmetry dependence of some of the physical observables and the results have been compared with the corresponding experimental data.

#### A. Fission shapes and Friction form factors

The evolution of fission shapes for the symmetric ( $\alpha = 0.0$ ) as well as asymmetric ( $\alpha = 0.15$ ) splitting of a representative compound system of mass  $A_{CN}=200$  are illustrated in Fig. 2. Fig. 2a to Fig. 2g represent the gradual evolution of the shape from the spherical ground state ( $c = 1$ ) to the scission point ( $c = c_{sc}$ ). It may be pointed out that the centre to centre separation at the scission point is  $\sim 18$  fm which is much larger than what one gets in the schematic shape of [23].

In the present calculations, a combination of both one-body and two-body frictions has been used to calculate the fission trajectories and the fission observables. In Fig. 3 form factors of the one-body and two-body frictions are displayed as a function of the centre to centre separation between the two symmetric fragments for a typical system of mass  $A_{CN} = 200$ . It is seen from Fig. 3 that at smaller separations (when the shape is nearly mononuclear), one-body friction is stronger whereas at larger separations, two-body friction dominates. However, one-body friction does not change much with the increase in separation between the fragments.

## B. Precission Neutron Multiplicities

As precission neutron multiplicities depend on time scale of the fission process and *vis-a-vis* on the magnitude of nuclear friction, theoretical estimates of the friction coefficients are usually made by reproducing the precission neutron multiplicity data using friction coefficient as an input parameter in the model. In the present calculations, one-body 'wall' friction has been used in the ground state to saddle region, where nuclear shapes are nearly mononuclear. The strength of the one-body friction used was attenuated to 10% of the original 'wall' value. This weakening of the wall friction has also been confirmed from the study of the role of chaos in dissipative nuclear dynamics [27]. In the saddle to scission region, on the other hand, the nuclear dissipation was taken to be of two-body origin. For the two-body friction, the viscous drag was calculated in the framework of Werner-Wheeler using Eqn. (8a) and the value of the viscosity coefficient  $\mu_0$  used in the present calculation was ( $4 \times 10^{-23} \text{MeV} \cdot \text{sec} \cdot \text{fm}^{-3}$ ). This value of  $\mu_0$  corresponds to 0.06 TP ( $1TP = 6.24 \times 10^{-23} \text{MeV} \cdot \text{sec} \cdot \text{fm}^{-3}$ ).

The calculated precission neutron multiplicities have been displayed in Fig. 4 as a function of the initial excitation energy of the compound nucleus for two different mass regions, *ie*, for  $A_{CN} \sim 150$  (*upper half*), and  $A_{CN} \sim 200$  (*lower half*). The solid curves represent the results of the present calculations and different symbols correspond to different sets of experimental data [3,4,6]. It is seen that for heavier systems ( $A_{CN} \sim 200$ ), the theoretical predictions are in good agreement with the corresponding experimental data. For lighter systems ( $A_{CN} \sim 150$ ), the experimental points are somewhat scattered and the theory is seen to reproduce quite well the average trend of the data. Here, the precission neutron multiplicities are less and the uncertainties are more which are reflected in the larger error bars of the experimental measurements. Moreover, as different experimental points belong to different compound nuclei (different symbols in the figure), additional fluctuations in neutron emission due to specific structure effects may not be ruled out. For example, compound system  $^{162}\text{Yb}$ , formed in the reaction  $^{18}\text{O} + ^{144}\text{Sm}$  (*filled diamond*), is quite neutron deficient compared to  $^{168}\text{Yb}$ , formed in the reaction  $^{18}\text{O} + ^{150}\text{Sm}$  (*open triangle*). Therefore, neutron emission from the former is expected to be somewhat less. In fact, such system dependent fluctuations of the average neutron multiplicities have also been observed when calculations were done for specific systems (see text below). At very high excitation energies, the observed multiplicity (*open diamond*) was found to be lower than the average theoretical trend. In this case, the incident energy was quite high ( $> 10 \text{ MeV/nucleon}$ ), and the onset of preequilibrium emission process may not be ruled out. As preequilibrium particles carry away a larger amount of energy compared to the evaporated particles, the fused composite cools down faster and subsequently leads to fewer emission of evaporated particles [3]. As preequilibrium emission has not been considered in the present calculation, the model predictions of multiplicities are expected to be somewhat higher than the experimental measurements of the same at higher bombarding energies.

In Fig. 5(a), we have plotted precission neutron multiplicities  $n_{pre}$  as function of the compound nuclear mass  $A_{CN}$  for 158.8 MeV  $^{18}\text{O}$  induced reactions on different targets. The solid curve represents the theoretical predictions whereas the filled circles correspond to the experimental data [3]. It is seen that the observed multiplicities increase with the increase in  $A_{CN}$  in general and show some fluctuations in the vicinity of  $A_{CN} \sim 160 - 170$ , in particular. The present calculations are found to be quite successful in reproducing the general trend of the data over the whole range of masses studied. The fluctuations in the observed multiplicities, which may be due to specific structure effects, as discussed earlier, have also been reproduced qualitatively in the present model.

It is interesting to note that the present model with a single value of friction coefficient,  $\mu_0$  has been able to explain the general trend of the data over the whole range of masses and excitation energies of the compound nuclei studied. This is similar to what one expects in the Werner-Wheeler prescription, which predicts that the reduced friction coefficient,  $\beta$  should be a universal function depending only on the collective degrees of freedom [25]. Earlier attempts, on the contrary, have shown that the values of the friction coefficients are system dependent and vary over a wide range (typically, the reduced friction coefficient,  $\beta$ , may have values between  $2 \times 10^{-21} \text{sec}^{-1}$  and  $20 \times 10^{-21} \text{sec}^{-1}$  [13]). However, Frobrich *et. al.* attempted to arrive at such a universal value of the  $\beta$  in the framework of modified Langevin equation model [14] by using the level density formula proposed by Ignatyuk *et. al.* [26]. They had to use a constant value of  $\beta$  ( $= 2 \times 10^{-21} \text{sec}^{-1}$ ) for the ground state to saddle followed by a set of  $\beta$  values proportional to the elongation parameter, which reaches upto a value of  $30 \times 10^{-21} \text{sec}^{-1}$  at the scission point in order to reproduce the experimental data.

## C. Energy of emitted neutrons and TKE

To have a closer look into the predictions of the present model so far as other related observables are concerned, the average energy of the precission neutrons,  $\langle E_n \rangle$  and total kinetic energy (TKE) of the fragments have been plotted as a function of the compound nuclear mass,  $A_{CN}$ , in Figs. 5(b) and 5(c), respectively. It is seen from the figure that the theoretical predictions for all the observables (*solid curve*) are in good agreement with the respective

experimental data (*filled circles*). The observed system dependent fluctuations of both  $\langle E_n \rangle$  and TKE are also, reproduced fairly well in the present calculations.

#### D. Fragment mass asymmetry dependence

Calculations have also been performed to reproduce the available experimental data for the asymmetric fission of the heavy mass compound systems. The systems studied for the asymmetric fission are the ones produced in  $^{18}O$  ( $E_{lab} = 158.8$  MeV) induced reactions on  $^{154}Sm$ ,  $^{197}Au$  and  $^{238}U$  [3]. Fig.6 shows the predicted precission neutron multiplicities  $n_{pre}$  (dashed curves), calculated with the same friction values as used in symmetric fission in the previous section, as a function of the fragment asymmetry, alongwith the corresponding experimental data (solid circles). It is evident from the figure that, for all the systems, the predicted values of  $n_{pre}$  are very weakly dependent on the fragment asymmetry, whereas the experimental values decrease rapidly with the increase in fragment asymmetry. It may be conjectured that the friction form factors calculated from the Werner-Wheeler prescription, which successfully explains the symmetric fission data, are rather inadequate in reproducing the experimental data in the case of asymmetric fission. It appears that the above friction form factors need some modification, ie, some extra asymmetry dependence should be included in the form factor to explain the asymmetric fission data. It has been found that, with the inclusion of a factor  $h(\alpha) = \exp(-K\alpha^2)$  in the expression for friction form factor (Eqn. 8a), the predicted values of  $n_{pre}$  (solid curves) agree quite well with the respective experimental data. The value of the constant  $K$  was found to be  $161 \pm 3$  which is independent of the mass of the compound system. It is, therefore, interesting to note that with the inclusion of this extra term  $h(\alpha)$ , we can still use the same value of the viscosity coefficient,  $\mu_0$ , as used earlier in Secs. III B, III C to explain the precission neutron multiplicity data for both symmetric as well as asymmetric fission.

We have also studied the variation of precission neutron multiplicities as well as the time scale of fission as function of the angular momentum. The Figs. 7(a, b) show the calculated results for fission time  $\tau_f$  and neutron multiplicities  $n_{pre}$ , respectively, for a typical system  $^{18}O+^{197}Au$  for different values of asymmetry parameter  $\alpha$ . It is clear from the figure that both  $n_{pre}$  and  $\tau_f$  have only a weak dependence on  $L$ . However, both these quantities have a strong dependence on fragment asymmetry and are found to decrease with the increase in fragment asymmetry. The time scales vary in the range of 0.5 to 1.5 ( $\times 10^{-20}$  sec.) as asymmetry parameter  $\alpha$  decreases from 0.1 to 0. A similar trend is observed in the variation of  $n_{pre}$ .

### IV. SUMMARY AND CONCLUSIONS

To sum up, we have developed a dynamical model for fission where fission trajectories are generated by solving Euler-Lagrange equations of motion using a combination of one- and two-body frictions. Evolution of shapes of the fissioning nuclei have been computed from the generalised shape parametrisation of Brack *et. al.* [24]. Different friction form factors have been used for ground state to saddle and saddle to scission regions. In the ground state to saddle region, the one body 'wall' friction has been used with an attenuation coefficient of 0.1, whereas the two body dissipative forces, derived from Werner-Wheeler prescription, have been used in the saddle to scission region with the value of the two body viscosity coefficient  $\mu_0 = 4 \times 10^{-23} \text{ MeV} \cdot \text{sec} \cdot \text{fm}^{-3}$ . Same values of the friction coefficients have been used for all the systems considered here. With these values of friction coefficients, the typical time scales of fission as obtained from the present calculations were  $\sim (1 - 2) \times 10^{-20}$  sec. for symmetric fission, which are similar to the values reported earlier in the literature. Emission of neutrons along the fission trajectories has been simulated through Monte-Carlo simulation technique. The evolution of the fission trajectories has been corrected for precission proton emission, which has been simulated in a similar way as it was done for neutron emission. However, the precission proton emission was found to be quite small compared to the neutron emission for the systems considered in the present studies. The emission of complex particles (d, t,  $^4\text{He}$  etc.) and their effects on precission neutron emission has been neglected in the present calculation as it is difficult to incorporate them in the present model because of their composite nature. Generally complex particle emission is much less as compared to the neutron emission; however, for some fissioning nuclei  $\alpha$  emission may be relatively favoured due to structure effects and it may affect the neutron multiplicity and other fission observables. Theoretical predictions for precission neutron multiplicities, total kinetic energies and the mean energies of the precission neutrons, for all the systems considered here, agree quite well with the corresponding available experimental data.

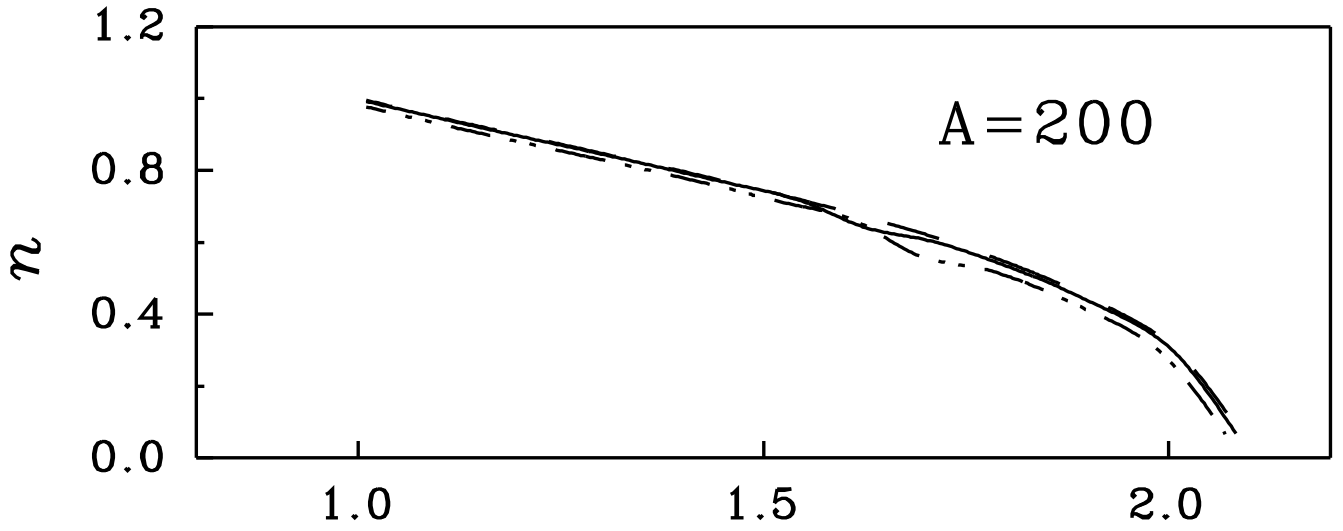
In the present model, the fragment mass asymmetry dependence of the precission neutron multiplicities and other physically relevant quantities have also been studied. It has been found that with the inclusion of an extra factor ( $\exp(-K\alpha^2)$ ,  $K=161\pm 3$ ) in the friction form factor (Eqn. 8a), the observed decrease of the precission neutron



multiplicities with the increase in fragment mass asymmetry, are explained fairly well with the same value of the viscosity coefficient  $\mu_0$  as used in the case of symmetric fission. Further, it has been observed that the precession neutron multiplicities as well as fission time are weakly dependent on the angular momentum of the fissioning system. However, the fission times are found to be strongly dependent upon the fragment mass asymmetry and decrease from 1.5 to 0.5 ( $\times 10^{-20}$  sec.) as the the asymmetry parameter  $\alpha$  increase from 0.0 to 0.1.

To conclude, in the present model, with the generalised shape parametrisation and modified Werner-Wheeler friction form factor, both symmetric and asymmetric splitting of the compound nucleus can be treated on the same footing. The present model is quite successful in explaining precession neutron multiplicities, total fragment kinetic energies, average energies of the precession neutrons, as well as their fragment mass asymmetry dependence.

- 
- \* Present address :: Institut de Recherches Subatomiques, IN2P3-CNRS/Universite Louis Pasteur, B.P. 28, F-67037 STRASBOURG CEDEX 2, France.
- [1] S. S. Kapoor, Proceedings of Consultants Meeting on Physics of Neutron Emission in Fission, Mito City, Japan (International Nuclear Data Committee) **220**, 221 (1989).
  - [2] D. J. Hilscher, H. Rossner, B. Cramer, B. Gebauer, U. Jahnke, M. Lehmann, E. Mordhorst, and W. Scobel, Phys. Rev. Lett. **62**, 1099 (1989).
  - [3] D. J. Hinde, D. Hilscher, H. Rossner, B. Gebauer, M. Lehmann, and M. Wilepert, Phys. Rev. C **45**, 1229 (1992).
  - [4] D. J. Hinde, R. J. Charity, G. S. Foote, J. R. Leigh, J. O. Newton, S. Ogaza, and A. Chatterjee, Nucl. Phys. A **452**, 550 (1986).
  - [5] J. O. Newton, D. J. Hinde, R. J. Charity, J. R. Leigh, J. J. M. Bokhorst, A. Chatterjee, G. S. Foote, and S. Ogaza, Nucl. Phys. A **483**, 126 (1988).
  - [6] A. Gavron, A. Gayer, J. Boissevain, H. C. Britt, T. C. Awes, J. R. Beene, B. Cheynis, D. Drain, R. L. Ferguson, F. E. Obenshain, F. Plasil, G. R. Young, G. A. Pettitt, and C. Butler, Phys. Rev. C **35**, 579 (1987).
  - [7] H. Rossner, D. J. Hinde, J. R. Leigh, J. P. Lestone, J. O. Newton, J. X. Wei, and S. Elfstrom, Phys. Rev. C **45**, 719 (1992).
  - [8] J. P. Lestone, J. R. Leigh, J. O. Newton, D. J. Hinde, J. X. Wei, J. X. Chen, S. Elfstrom, and D. G. Popescu, Phys. Rev. Lett. **67**, 1078 (1991).
  - [9] A. Saxena, A. Chattejee, R. K. Choudhury, S. S. Kapoor, and D. M. Nadkarni, Phys. Rev. C **49**, 932 (1994).
  - [10] W. Schmid, T. von Egidy, F. J. Hartmann, J. Hoffmann, S. Schmid, D. Hilscher, D. Polster, H. Rossner, A. S. Iljinov, M. V. Mebel, D. I. Ivanov, V. G. Nedorezov, A. S. Sudov, H. Machner, H. S. Plendl, J. Eades, S. Neumaier, Phys. Rev. C **55**, 2965 (1997).
  - [11] Y. Abe, C. Gregoire, and H. Delagrang, J. Phys. (Paris) **47**, 32 (1986).
  - [12] Y. Abe, S. Ayik, P. G. Reinhard, and E. Suraud, Phys. Rep. **275**, 49 (1996) and references therein.
  - [13] N. D. Mavlitov, P. Frobrich, and I. I. Gontchar, Z. Phys. A **342**, 195 (1992).
  - [14] P. Frobrich, I. I. Gontchar, and N. D. Mavlitov, Nucl. Phys. A **556**, 281 (1993).
  - [15] K. Pomorski, J. Bartel, J. Richert, and K. Dietrich, Nucl. Phys. A **605**, 87 (1996).
  - [16] A. Kramers, Physica **7**, 284 (1940).
  - [17] P. Grange, Li Jun-Qing, and H. A. Weidenmuller, Phys. Rev. C **27**, 2063 (1983).
  - [18] E. Strumberger, K. Dietrich, and K. Pomorski, Nucl. Phys. A **521**, 522 (1991).
  - [19] K. T. R. Davies, A. J. Sierk, and J. R. Nix, Phys. Rev. C **13**, 2385 (1976).
  - [20] H. Feldmeier, Rep. Prog. Phys. **50**, 915 (1987).
  - [21] Asish K. Dhara, C. Bhattacharya, S. Bhattacharya, and K. Krishan, Phys. Rev. C **48**, 1910 (1993).
  - [22] C. Bhattacharya, S. Bhattacharya, and K. Krishan, Phys. Rev. C **53**, 1012 (1996).
  - [23] W. J. Swiatecki, in progress in particle and Nuclear Physics, edited by D. Wilkinson (Pergamon, New York, 1980), Vol. 4, pp. 383; J. Randrup, Nucl. Phys. A **307**, 319 (1978).
  - [24] M. Brack, J. Damgard, A. S. Jensen, H. C. Pauli, V. M. Strutinsky, and C. Y. Wong, Rev. Mod. Phys. **44**, 320 (1972).
  - [25] I. I. Gontchar, G. I. Kosenko, N. I. Pischasov, and O. I. Serdyuk, Sov. J. Nucl. Phys. **55**, 514 (1992).
  - [26] A. V. Ignatyuk, M. G. Itkis, V. N. Okolovich, G. N. Smirenkin, and A. S. Tishin, Yad. Fiz. **21**, 1185 (1975).
  - [27] S. pal, Pramana-J. Phys., **48**, 425 (1997).



C

FIG. 1. Variation of neck radius  $n$  with  $c$  for different values of the parameter  $\alpha$ . Dash, solid and dash-dot lines correspond to  $\alpha=0, 0.05$  and  $0.10$ , respectively.

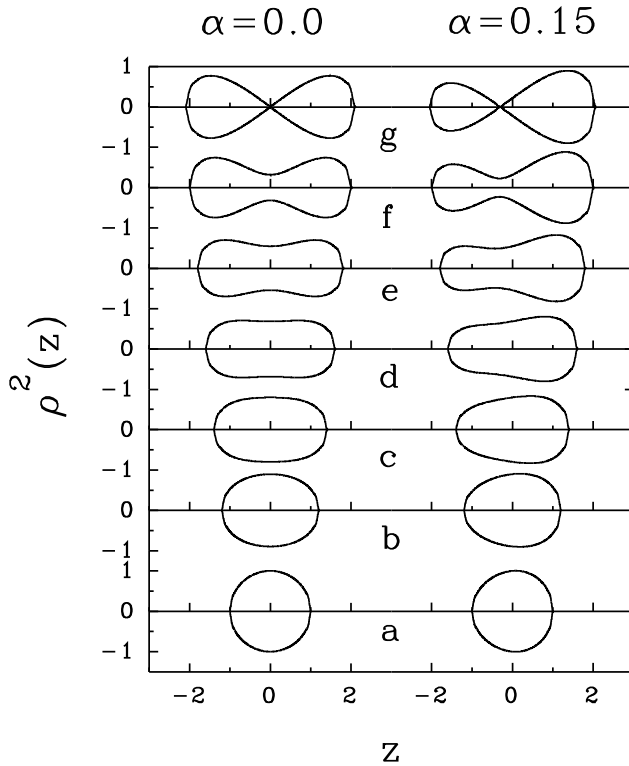


FIG. 2. Evolution of fission shapes for a compound system of mass  $A_{CN} = 200$  for  $\alpha = 0.0$  and  $0.15$ . Figs. (a) to (g) represent the shapes of the fissioning shapes for  $c = 1, 1.2, 1.4, 1.6, 1.8, 2.0$  and  $c_{sc}$ , respectively. 'Negative' values of  $\rho^2$  are the mirror reflection of the upper half about the elongation axis.

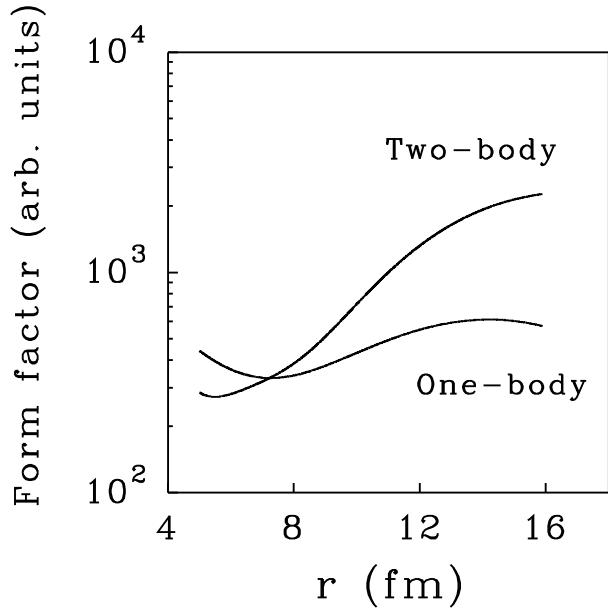


FIG. 3. Friction form factors for one-body and two-body frictions plotted as a function of the centre to centre separation  $r$  between the two symmetric fragments for a compound system of mass  $A_{CN} = 200$ .

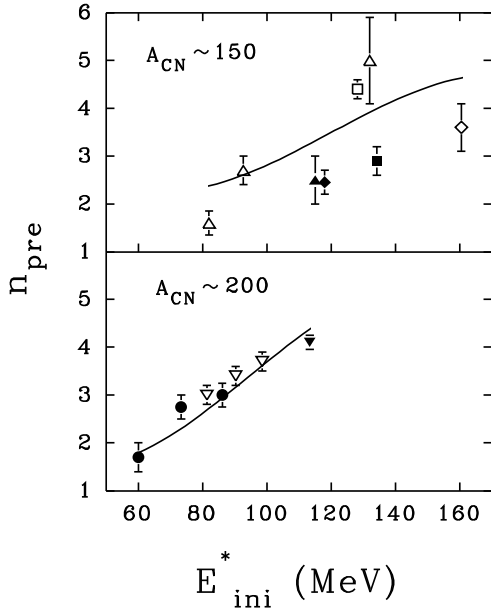


FIG. 4. Precission neutron multiplicities plotted as a function of the initial excitation energy  $E_{ini}^*$  of the compound nuclei of masses  $A_{CN} \sim 150$  (*upper half*), and  $A_{CN} \sim 200$  (*lower half*). The solid curve is the present calculation. Different symbols correspond to different sets of experimental data, (*ie*, filled circle  $\rightarrow$   $^{28}\text{Si}+^{170}\text{Er}$  [4], open inverted triangle  $\rightarrow$   $^{19}\text{F}+^{181}\text{Ta}$  [4], filled inverted triangle  $\rightarrow$   $^{18}\text{O}+^{197}\text{Au}$  [3], open triangle  $\rightarrow$   $^{18}\text{O}+^{150}\text{Sm}$  [4], filled triangle  $\rightarrow$   $^{24}\text{Mg}+^{134}\text{Ba}$  [6], open diamond  $\rightarrow$   $^{16}\text{O}+^{142}\text{Nd}$  [6], filled diamond  $\rightarrow$   $^{18}\text{O}+^{144}\text{Sm}$  [3], open square  $\rightarrow$   $^{18}\text{O}+^{154}\text{Sm}$  [3], filled square  $\rightarrow$   $^{18}\text{O}+^{124}\text{Sn}$  [3]).

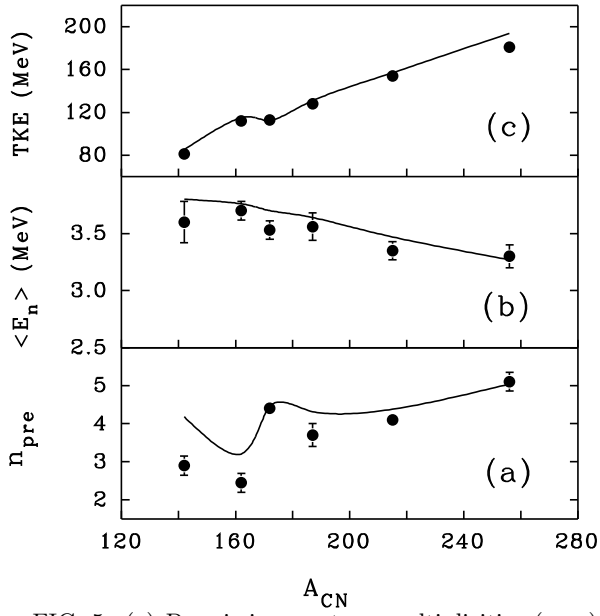


FIG. 5. (a) Precission neutron multiplicities ( $n_{pre}$ ), (b) mean energy of the evaporated neutrons ( $\langle E_n \rangle$ ) and (c) total kinetic energy of the fragment (TKE), plotted as a function of  $A_{CN}$ . The solid curves are the present calculations, and the filled circles are the corresponding data [3].

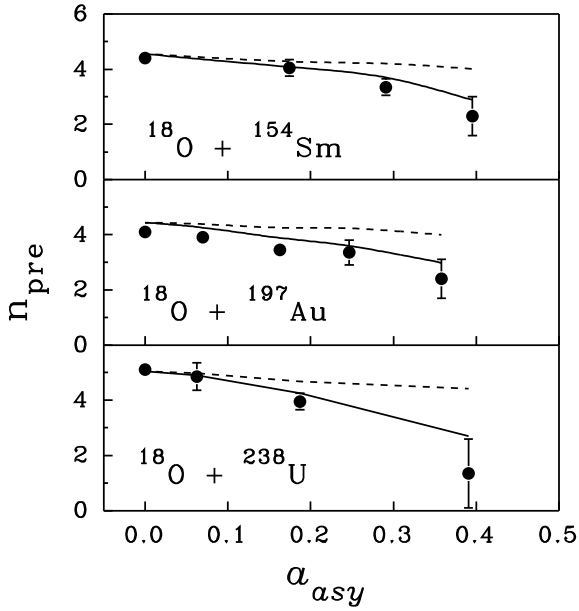


FIG. 6. Precission neutron multiplicity  $n_{pre}$  as a function of fragment mass asymmetry  $a_{asy}$  for  $^{18}\text{O}$  induced reactions on  $^{154}\text{Sm}$ ,  $^{197}\text{Au}$  and  $^{238}\text{U}$ . Filled circles correspond to the experimental data [3]. The dash curves represent the calculated results with friction form factors of  $8a$  and the solid curves represent the calculated results with modified friction form factors (*see text*).

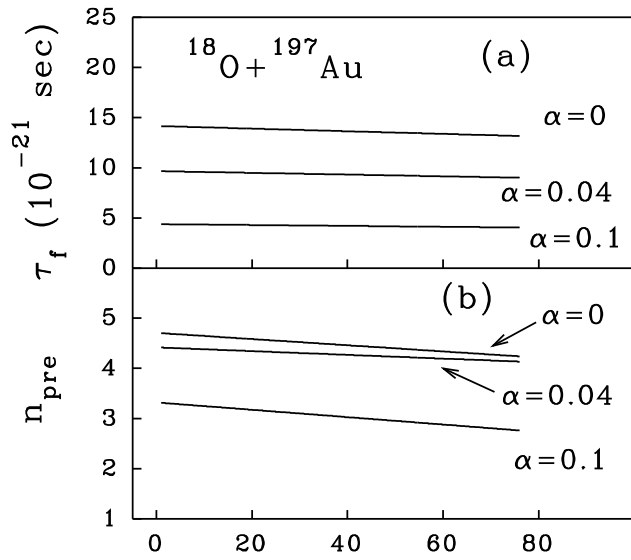


FIG. 7. Theoretical predictions of (a) Fission time  $\tau_f$ , and (b) precission neutron multiplicities  $n_{pre}$  plotted as a function of angular momentum  $L$  for the reaction 158.8 MeV  $^{18}\text{O}$  on  $^{197}\text{Au}$  for different values of the asymmetry parameter  $\alpha$ .